



# On the observation of Solar System Small Bodies with the SST telescopes

Caetano E. H. O.<sup>1</sup>, Sobrinho J. L. G.

July 2023

Grupo de Astronomia da Universidade da Madeira  
Faculdade de Ciências Exatas e da Engenharia  
Universidade da Madeira, Campus da Penteada, 9020-105 Funchal  
astro@uma.pt  
<https://astro.web.uma.pt/Grupo/index.htm>

## Abstract

The project Space Surveillance and Tracking (SST) aims to do the monitoring and tracking of space debris in Earth's orbit. At Pico do Areeiro on the Madeira Autonomous Region the project has two optical telescopes: one for tracking operations and the other for surveillance operations. Although these telescopes are dedicated to the detection of space debris, they can be used in the field of Observational Astronomy. In this work we discuss the observation of Solar System Small Bodies (SSSBs) using the SST telescopes. After doing a survey of the main SSSBs belonging to different groups according to their orbital characteristics (Atiras, Amors, Atens, Apollos, Main Belt, Trojans, Centaurs, Transneptunians and Plutinos) we determine, for a selection of them, the SST telescopes exposure times. At the end we present an observation proposal for nine of the considered objects. We concluded that the capabilities of the SST equipments are well enough to observe and track most of the considered objects and dwarf planets as well.

**Keywords:** Asteroid(Minor Planet) - Dwarf Planets - Declination - Right Ascension - Magnitude - Observations - Signal to Noise

## 1 Introduction

The Space Surveillance and Tracking (SST) program has as its central objective the monitoring and tracking of space debris in Earth orbit that are potentially dangerous for space infrastructure, for access to space as well as for the safety of populations. The SST project, under the responsibility of the Ministry of National Defense (MDN), has installations in mainland Portugal, in the Autonomous Region of Azores and in the Autonomous Region of Madeira (RAM). At Pico do Areeiro (RAM) the project has two optical telescopes: one for tracking operations and the other for surveillance operations (Freitas et al., 2021).

---

<sup>1</sup>Caetano E. H. O. was supported by the **Estágios de Verão 2023** programme, promoted by the **Secretaria Regional da Educação**, through the **Direção Regional de Juventude e Desporto (DRJD)** - Região Autónoma da Madeira.

Table 1: The SST telescopes and corresponding CCD's.

Parameter	Surveillance	Tracking	Ref.
Telescope aperture	356 mm	400 mm	(Freitas et al., 2021)
CCD chip	GSense4040	EMCCD 201 e2v Back-illuminated	(Freitas et al., 2021)
CCD array	$4096 \times 4096$	$1024 \times 1024$	(Freitas et al., 2021)
Field of view	$2.67^\circ \times 2.67^\circ$	$0.35^\circ \times 0.35^\circ$	(Freitas et al., 2021)
Quantum Efficiency	73%	90%	(Freitas et al., 2021)
Read noise	$3.7 \text{ e}^- \text{pix}^{-1}$	$< 1 \text{ e}^- \text{pix}^{-1}$	(Gpixel, 2023; EMCCD, 2023)
Dark current	$12.2 \text{ e}^- \text{s}^{-1} \text{pix}^{-1}$	$0.00025 \text{ e}^- \text{s}^{-1} \text{pix}^{-1}$ ( $-80^\circ\text{C}$ )	(Gpixel, 2023; EMCCD, 2023)

The University of Madeira (UMa), through its Astronomy Group (GAUMa), currently provides support/maintenance services to the installed equipments. In addition GAUMa is allowed to run its own observation program interspersed with the SST observations. As a matter of fact, although the installed telescopes are dedicated to detecting space debris, they have the necessary technical requirements so that they can be used in the field of Observational Astronomy (Freitas et al., 2021; Sobrinho, 2022). In Table 1 we show some of the characteristics of the two telescopes/CCD's operating within the SST project in Madeira.

One of the fields in which SST telescopes can be used is in the observation and tracking of the so called Solar System Small Bodies (SSSBs). On it's Resolution B5 (Definition of a Planet in the Solar System) the International Astronomic Union (IAU) establishes that a SSSB is an object in the Solar System that is neither a planet, a dwarf planet, nor a natural satellite. These currently include most of the Solar System asteroids, most Transneptunian Objects (TNOs), comets, and other small bodies (IAU, 2006).

In this work we explore the potential of using the SST telescopes in the observation of SSSBs including asteroids of different families as well as Kuiper Belt Objects (KBOs). We considered the five dwarf planets identified to date given the close relationship between them and SSSBs.

In section Section 2 we present a survey of the main asteroids and KBO's grouped according to their orbital characteristics, in Section 3 we determine which objects can be observed using the SST telescopes and in Section 4 we present an observing program for the summer of 2023. Finally, in Section 5, we present some conclusions and ideas for future work.

## 2 Solar System Small Bodies

One way of classifying SSSBs consists on taking into account their location within the Solar System as well as their orbit parameters (e.g. aphelion and perihelion). Asteroids are rocky objects mostly located on the so-called Main Belt between the orbits of Mars and Jupiter. However asteroids could also be found outside the Main Belt region, for example, in the Inner Solar System. In this work we have considered asteroids from six different orbital families:

- Atiras ( $a < 0.983$  AU) - Table 2
- Atens ( $0.983 < a < 1$  AU) - Table 3,
- Apollos ( $1 < a < 1.017$  AU) - Table 4,
- Amors ( $1.017 < a < 1.3$  AU) - Table 5,
- Main Belt ( $2.06 < a < 3.27$  AU) - Table 6,
- Trojans ( $\approx 5.2$  AU) - Table 7.

Table 2: Main characteristics of the biggest Atiras, including the perihelion (q), aphelion(Q), absolute magnitude (H), orbital period (P), relative velocity (V) and diameter (D). Data was taken from the Minor Planet Center database (MPC, 2023)

Name	q (AU)	Q (AU)	H	P (days)	V (km/s)	D (km)
594913' Aylo'chaxnim	0.457	0.654	16.2	151	40.01	1.996
163693 Atira	0.502	0.980	16.3	233	34.60	1.809
2008 EA32	0.428	0.804	16.5	177	37.86	1.728
2019 LF6	0.317	0.790	17.3	151	40.01	1.201
2019 AQ3	0.404	0.774	17.5	165	38.82	1.090
2005 TG45	0.428	0.935	17.6	205	36.16	1.022
2018 JB3	0.485	0.882	17.7	206	36.08	1.008
2021 PH27	0.133	0.794	17.7	115	43.68	0.990
2021 VR3	0.313	0.755	18.0	143	40.63	0.846
2017 YH	0.328	0.940	18.4	185	37.31	0.741

In each case we have selected the 10 biggest asteroids. All the data presented on Tables 2-7 was retrieved directly from the Minor Planet Center (MPC) (MPC, 2023). Notice that the absolute magnitude, represented by  $H$ , is defined as the apparent magnitude that a SSSB would have if it was located at a distance of 1 AU away from both the observer and the Sun, and in conditions of solar opposition. We should not confuse this absolute magnitude  $H$  with the absolute magnitude  $M$  usually used for stars (see Appendix A).

A SSSB between the orbits of Jupiter and Neptune is called a Centaur, and a SSSB beyond the orbit of Neptune is referred to as a Transneptunian object (TNO). This means that a KBO is also a TNO. In this work we have considered:

- Centaurs ( $q > 5.2$  and  $a < 30.1$  AU) - Table 8,
- Transneptunian ( $a > 30.1$  AU) - Table 9,
- Plutinos ( $a > 30.1$  AU, with a resonance 2:3 with Neptune) - Table 10.

In each case we have selected the 10 biggest objects. All the data presented on Tables 8-10 was retrieved directly from the MPC (MPC, 2023).

Since the dwarf planet Ceres is located well within the Main Belt and the other four known dwarf planets belong to the Kuiper Belt we decided to include them in our work (cf. Table 11). We also grouped several Potentially Hazardous Asteroids (PHA) belonging to other asteroid categories into Table 12. This was done in order to better keep track of the objects that are bigger than 140 m in diameter and are, at some point during their orbit, at a distance to the Earth closer than 0.05 AU ( $\approx 20$  lunar distances).

### 3 Estimating the exposure time

The **signal-to-noise ratio** (SNR) measures how well an object is measured by comparing the signal received from the object,  $N_{obj}$ , with the total noise  $N$  (Howell, 2000):

$$SNR = \frac{N_{obj}}{N} \tag{1}$$

Table 3: Main characteristics of the biggest Atens, including the perihelion (q), aphelion(Q), absolute magnitude (H), orbital period (P), relative velocity (V) and diameter (D). Data was taken from the Minor Planet Center database (MPC, 2023)

Name	q (AU)	Q (AU)	H	P (days)	V (km/s)	D (km)
3554 Amun	0.70	1.25	15.91	351	30.19	3.341
2100 RA-Shalom	0.47	1.20	16.23	277	32.68	2.300
3753 Cruithne	0.48	1.51	15.5	364	29.82	2.071
66391 Moshup	0.20	1.08	16.64	188	37.17	1.317
2062 Aten	0.79	1.14	17.11	347	30.32	1.100
5381 Sekhmet	0.67	1.23	16.75	337	30.59	0.935
3362 Khufu	0.53	1.45	18.52	360	29.90	0.700
136818 Selqet	0.61	1.26	18.98	332	30.72	0.549
2340 Hathor	0.46	1.22	20.32	283	32.44	0.300
326290 Akhenaten	0.49	1.27	21.83	301	31.77	0.148

Table 4: Main characteristics of the biggest Apollos including the perihelion (q), aphelion(Q), absolute magnitude (H), orbital period (P), relative velocity (V) and diameter (D). Data was taken from the Minor Planet Center database (MPC, 2023)

Name	q (AU)	Q (AU)	H	P (years)	V (km/s)	D (km)
1866 Sisyphus	0.874	2.913	12.55	2.61	13.6	8.480
7092 Cadmus	0.774	4.310	15.13	4.05	8.9	6.319
3200 Phaethon	0.140	2.403	14.4	1.43	15.3	6.250
2212 Hephaistos	0.351	3.969	13.52	3.17	10.3	5.700
5143 Heracles	0.419	3.251	14.10	2.49	9.6	4.843
2329 Orthos	0.834	3.985	14.57	3.74	9.8	4.202
1864 Daedalus	0.563	2.358	14.88	1.77	10.3	3.700
4183 Cuno	0.721	3.241	14.18	2.79	7.4	3.651
1685 Toro	0.771	1.964	14.34	1.60	6.7	3.400
4197 Morpheus	0.522	4.066	15.03	3.48	9.3	1.800

Table 5: Main characteristics of the biggest Amors, including the perihelion (q), aphelion(Q), absolute magnitude (H), orbital period (P), relative velocity (V) and diameter (D). Data was taken from the Minor Planet Center database (MPC, 2023)

Name	q (AU)	Q (AU)	H	P (years)	V (km/s)	D (km)
1036 Ganymed	1.245	4.087	9.26	4.35	10.4	37.675
3552 Don Quixote	1.245	7.284	13.07	8.81	11.9	19.000
433 Eros	1.133	1.783	10.41	1.76	6.9	16.840
4954 Eric	1.102	2.901	12.56	2.83	7.7	10.800
1627 Ivar	1.124	2.602	12.85	2.54	6.3	9.120
1917 Cuyo	1.063	3.237	14.40	3.15	9.1	5.700
3122 Florence	1.020	2.517	14.10	2.35	8.2	4.900
5626 Melissabrucker	1.196	3.192	14.35	3.25	6.7	4.629
1980 Tezcatlipoca	1.086	2.333	13.87	2.24	9.5	4.300
887 Alinda	1.061	3.884	13.88	3.89	7.1	4.200

Table 6: Main characteristics of the biggest Main Belt asteroids, including the perihelion (q), aphelion(Q), absolute magnitude (H), orbital period (P), relative velocity (V) and diameter (D). we also include here the dwarf planet Ceres because it is located well within the Main Belt (and until 2006 it was considered an asteroid). Data was taken from the Minor Planet Center database (MPC, 2023)

Name	q (AU)	Q (AU)	H	P (years)	V (km/s)	D (km)
1 Ceres	2.55	2.99	3.33	4.60	17.92	939.400
4 Vesta	2.15	2.57	3.21	3.64	19.33	525.400
2 Pallas	2.13	3.41	4.12	4.60	17.94	513.000
10 Hygiea	2.79	3.49	5.6	5.56	16.83	407.120
704 Interamnia	2.58	3.54	6.29	5.34	17.07	306.313
52 Europa	2.75	3.44	6.57	5.45	16.91	303.918
511 Davida	2.56	3.76	6.43	5.61	16.77	270.327
87 Sylvia	3.15	3.80	6.98	6.49	15.97	253.051
15 Eunomia	2.15	3.14	5.38	4.30	18.31	231.689
624 Hektor	5.15	5.39	7.45	12.10	12.97	225.000

Table 7: Main characteristics of the biggest Jupiter Trojans, including the perihelion (q), aphelion(Q), absolute magnitude (H), orbital period (P), relative velocity (V) and diameter (D). Data was taken from the Minor Planet Center database (MPC, 2023)

Name	q (AU)	Q (AU)	H	P (years)	V (km/s)	D (km)
617 Patroclus	4.48	5.94	8.18	11.88	13.06	140.362
911 Agamemnon	4.92	5.64	7.99	12.13	12.97	131.038
3451 Mentor	4.79	5.56	8.49	11.77	13.09	126.288
3317 Paris	4.55	5.90	8.47	11.96	13.02	118.790
1867 Deiphobus	4.90	5.37	8.45	11.64	13.14	118.220
1172 Aeneas	4.67	5.79	8.30	11.96	13.02	118.020
1437 Diomedes	4.98	5.46	8.26	11.91	13.05	117.786
1143 Odysseus	4.76	5.72	8.38	11.99	13.01	114.624
3063 Makhaon	4.91	5.53	8.62	11.94	13.02	111.655
4709 Ennomos	5.14	5.39	8.68	12.10	12.97	91.433

Table 8: Main characteristics of the biggest Centaurs, including the perihelion (q), aphelion(Q), absolute magnitude (H), orbital period (P), relative velocity (V) and diameter (D). Data was taken from the Minor Planet Center database (MPC, 2023)

Name	q (AU)	Q (AU)	H	P (years)	V (km/s)	D (km)
10199 Chariklo	13.15	18.45	6.55	62.70	7.51	302.00
95626	18.01	28.19	7.18	111.16	6.19	230.50
5145 Pholus	8.69	31.91	7.07	91.41	6.61	190.00
2060 Chiron	8.55	18.87	5.66	50.65	8.06	166.00
562274	17.35	38.19	6.91	146.8	5.65	142.39
447178	13.88	43.84	7.30	154.96	5.55	118.98
463368	20.19	38.31	7.30	158.25	5.51	118.98
2002 TZ300	6.21	50.29	7.33	150.03	5.61	117.35
471149	18.00	26.90	7.43	106.50	6.28	112.60
55576 Amycus	15.25	34.83	7.44	125.39	5.95	100.90

Table 9: Main characteristics of the biggest TNOs, including the perihelion (q), aphelion(Q), absolute magnitude (H), orbital period (P), relative velocity (V) and diameter (D). The dwarf planets Eris, Makemake and Haumea were also included taking into account that by definition they are also TNOs. Dwarf planet Pluto, which is also a TNO, was included in table 10 with other plutinos. Data was taken from the Minor Planet Center database (MPC, 2023)

Name	q (AU)	Q (AU)	H	P (years)	V (km/s)	D (km)
136199 Eris	38.71	97.59	-1.21	561.26	3.62	5990.725
136472 Makemake	37.74	52.78	-0.2	303.90	4.44	3762.525
136108 Haumea	34.33	51.49	0.23	282.00	4.53	3086.593
90377 Sedna	76.39	988.21	1.54	12,292.95	1.29	1688.413
225088 Gonggong	33.77	100.79	1.86	553.05	3.62	1457.066
90482 Orcus	30.18	40.06	2.19	244.76	4.76	1251.640
50000 Quaoar	41.69	45.25	2.42	287.47	4.50	1125.847
532037	35.20	81.92	3.15	449.01	3.88	804.414
174567 Varda	39.11	52.43	3.46	309.38	4.41	697.396
28978 Ixion	29.81	49.39	3.47	249.14	4.73	694.192

Table 10: Main characteristics of the biggest Plutinos, including the perihelion (q), aphelion(Q), absolute magnitude (H), orbital period (P), relative velocity (V) and diameter (D). We also include here the dwarf planet Pluto because it is also a Plutino. Data was taken from the Minor Planet Center database (MPC, 2023)

Name	q (AU)	Q (AU)	H	P (years)	V (km/s)	D (km)
Pluto	29.58	49.32	-0.45	247.78	4.74	4221.622
208996	32.32	46.40	3.77	246.95	4.75	604.616
84922	36.40	42.72	4.01	248.87	4.73	541.352
455502	30.73	48.17	4.34	247.78	4.74	465.028
38628 Huya	28.55	50.15	4.8	246.68	4.75	376.252
47171	30.56	48.98	4.94	250.79	4.72	352.760
469372	35.53	43.77	5.34	249.69	4.73	293.413
55638	27.94	50.90	5.59	247.50	4.74	261.505

Table 11: Main characteristics of all the Dwarf Planets (known to date), including the perihelion (q), aphelion(Q), absolute magnitude (H), orbital period (P), relative velocity (V) and diameter (D). Data was taken from the Minor Planet Center database (MPC, 2023)

Name	q (AU)	Q (AU)	H	P (years)	V (km/s)	D (km)
136199 Eris	38.71	97.59	-1.21	561.26	3.62	5990.725
Pluto	29.58	49.32	-0.45	247.78	4.74	4221.622
136472 Makemake	37.74	52.78	-0.2	303.90	4.44	3762.525
136108 Haumea	34.33	51.49	0.23	282.00	4.53	3086.593
1 Ceres	2.55	2.99	3.33	4.6	17.92	939.400

Table 12: Main characteristics of the biggest Potentially Hazardous Asteroids (PHA) , including the perihelion (q), aphelion(Q), absolute magnitude (H), orbital period (P), relative velocity (V) and diameter (D). Data was taken from the Minor Planet Center database (MPC, 2023)

Name	q (AU)	Q (AU)	H	P (years)	V (km/s)	D (km)
3200 Phaethon	0.140	2.403	14.4	1.43	15.3	6.250
89830	1.02	3.13	14.99	2.98	20.73	5.067
3122 Florence	1.020	2.517	14.10	2.35	8.2	4.900
16960	0.31	4.09	14.42	3.26	20.11	4.482
4183 Cuno	0.721	3.241	14.18	2.79	7.4	3.651
4953	0.56	2.69	14.88	2.06	23.39	3.626
1981 Midas	0.62	2.93	15.28	2.37	22.35	3.400
111253	0.92	2.52	15.26	2.32	22.50	3.006
242450	0.57	1.60	14.62	1.13	28.62	2.914
1620 Geographos	0.83	1.66	15.32	1.39	26.68	2.560

Notice that a source might be bright but indistinguishable from the total noise, if the noise is high. Conversely, a faint source might be visible if the noise is low. This means that it is important to know not only the signal from the source but also the SNR value in order to determine whether the object will be visible or not in an image. Some SNR typical values (Hainaut, 2005):

- 2-3 : object barely detected
- 5 : object detected, one can really start to believe what one sees
- 10 : we can start to do measurements
- 100 : excellent measurement.

We may consider four different kinds of noise sources that could contribute with less or more extent to the total noise (Dhillon, 2010):

- $\sqrt{N_{obj}}$  - the photon noise from the **object** being observed (star or other object)
- $\sqrt{N_{sky}}$  - the photon noise from the **sky background**
- $\sqrt{N_{dark}}$  - the dark noise or **dark current** which consists on electrons thermally generated inside the CCD
- $R$  - the **read noise** generated by the CCD during each read

Assuming that all these noise sources are independent from each other then the total noise  $N$  will be given by (Dhillon, 2010):

$$N = \sqrt{N_{obj} + N_{sky} + N_{dark} + R^2} \quad (2)$$

Inserting equation (2) into equation (1) we get:

$$SNR = \frac{N_{obj}}{\sqrt{N_{obj} + N_{sky} + N_{dark} + R^2}} \quad (3)$$

In practice, we don't detect all the photons arriving at the CCD detector, only a fraction of them are converted into electrons and detected: this ratio electron/photon is called the **quantum efficiency** (QE) (Hainaut, 2005).

To use equation (3) correctly, one must assure that all the terms in the equation are expressed on the same unit system. Since inside the CCD photons counts arriving from the outside are ultimately converted into electron counts and that the noise generated inside the CCD are already expressed in electron counts we will assume that all the terms in equation (3) should be given in electron counts.

### 3.1 Noise from the object

In order to express the noise received from the object  $N_{obj}$  in terms of electrons we will start by considering how to express this quantity in photons per second.

Consider a star (or other object) of apparent magnitude  $m$  at a distance  $d = 10$  pc. In that case the corresponding absolute magnitude  $M$  will be equal to the apparent magnitude  $m$  since:

$$m - M = 5 \log \left( \frac{d}{10 \text{ pc}} \right) \quad (4)$$

Knowing the absolute magnitude we can determine the luminosity of the star  $L_*$  according to the relation:

$$M = M_{\odot} - 2.5 \log \left( \frac{L_*}{L_{\odot}} \right) \quad (5)$$

The brightness of the star can then be written as:

$$b = \frac{L_*}{4\pi d^2} \quad (6)$$

where we are considering that  $d = 10$  pc. Notice that if the distance to the star is not equal to 10 pc then we will obtain a different value for the luminosity. However the value of  $b$  will be always the same. In this context we can regard  $L_*$  as some kind of *virtual luminosity*.

The value of  $b$  gives us the amount of energy per unit time per unit area reaching the telescope. Thus the amount of energy per unit time will be:

$$E_{obj} = b\pi \left(\frac{D}{2}\right)^2 \quad (7)$$

where  $D$  is the aperture (diameter) of the telescope. Now we need to convert this flux of energy to photons per second. In the case of a monochromatic signal it is straightforward that the number of photons  $n$  will be given by:

$$n = \frac{E_{obj}}{h\nu} = \frac{E_{obj}\lambda}{hc} \quad (8)$$

Here we will estimate the true value of  $S_{obj}$  doing the average:

$$S_{obj} = \frac{n_{red} + n_{blue}}{2} = \frac{E_{obj} \lambda_{red} + \lambda_{blue}}{hc} \quad (9)$$

Finally, the value of  $N_{obj}$  expressed in electrons can be written as:

$$N_{obj} = S_{obj} \times t \times QE \quad (10)$$

where  $S_{obj}$  represents the number of photons per second received from the object,  $t$  is the exposure time and  $QE$  the CCD's quantum efficiency.

- **Example:** Consider a  $m = 18$  star. Let us assume that the distance to this star is  $d = 10$  pc. In that case the absolute magnitude of the star will be  $M = m = 18$  (equation 4). From equation (5) with  $M_{\odot} = 4.83$  and  $L_{\odot} = 3.828 \times 10^{26} \text{ Js}^{-1}$  we get for the star's luminosity  $L_* \approx 8.26 \times 10^{21} \text{ Js}^{-1}$ . If 10 pc corresponds to the true distance to the star then this will be the star's luminosity. Otherwise  $L_*$  can be regarded as a virtual luminosity.

Inserting  $L_*$  into equation (6) with  $d = 10$  pc we get  $b \approx 1.71 \times 10^{-15} \text{ Js}^{-1}\text{m}^{-2}$ .

This flux could be converted from  $\text{Js}^{-1}\text{m}^{-2}$  into  $\text{Js}^{-1}$  if we multiply it by the effective area of the telescope in use. In the case of the surveillance telescope we have  $D = 356$  mm (cf. Table 1). Inserting  $b$  and  $D$  into equation (7) we get  $E_{obj} \approx 1.71 \times 10^{-16} \text{ Js}^{-1}$ . This value can now be converted to  $\text{phs}^{-1}$  with the help of equation (9) giving:

$$S_{obj} = \frac{1.71 \times 10^{-16}}{6.626 \times 10^{-34} \times 3 \times 10^8} \frac{400 \times 10^{-9} + 700 \times 10^{-9}}{2} \approx 471 \text{ phs}^{-1}$$

For an exposure time of 10 s and a quantum efficiency of 73% (cf. Table 1) we get  $N_{obj} = 471 \times 10 \times 0.73 \approx 3438$  electrons.

In Table 13 we show  $S_{obj}$  (equation 9) for different values of  $m$  for both the surveillance and tracking telescopes. The values were determined following the same steps as explained on the  $m = 18$  star example.

Table 13: The number of photons per second ( $S_{obj}$ ) reaching the surveillance and tracking telescopes as a function of the apparent magnitude (m) of the object.

m	$S_{obj-surv}$ (phs $^{-1}$ )	$S_{obj-track}$ (phs $^{-1}$ )
1	$2.972 \times 10^9$	$3.752 \times 10^9$
2	$1.183 \times 10^9$	$1.494 \times 10^9$
3	$4.710 \times 10^8$	$5.946 \times 10^8$
4	$1.875 \times 10^8$	$2.367 \times 10^8$
5	$7.465 \times 10^7$	$9.424 \times 10^7$
6	$2.972 \times 10^7$	$3.752 \times 10^7$
7	$1.183 \times 10^7$	$1.494 \times 10^7$
8	$4.710 \times 10^6$	$5.946 \times 10^6$
9	$1.875 \times 10^6$	$2.367 \times 10^6$
10	746481	942407
11	297179	375179
12	118309	149361
13	47099.7	59461.90
14	18750.7	23672.20
15	7464.81	9424.07
16	2971.79	3751.79
17	1183.09	1493.61
18	471.00	594.62
19	187.51	236.72
20	74.65	94.24
21	29.72	37.52
22	11.83	14.94
23	4.71	5.95
24	1.88	2.37
25	0.746	0.942
26	0.297	0.375
27	0.118	0.149
28	0.0471	0.0595
29	0.0188	0.0237
30	0.00746	0.00942

Table 14: The number of photons per second and per pixel from the background sky ( $S_{sky}$ ) reaching the surveillance and tracking CCD's as a function of the sky background brightness ( $s$ ).

$s$ (msas)	$S_{sky-surv}$ (phs <sup>-1</sup> pix <sup>-1</sup> )	$S_{sky-track}$ (phs <sup>-1</sup> pix <sup>-1</sup> )
16	16365.4	367.84
17	6515.18	146.44
18	2593.74	58.30
19	1032.59	23.21
20	411.08	9.24
21	163.65	3.68
22	65.15	1.46
23	25.94	0.58

### 3.2 Noise from the background sky

The Sky Quality Meter (SQM) is a sensor that measures the sky background brightness ( $s$ ) in units of magnitudes per square arc second (msas). A measure giving  $s = 20$  msas, for example, tell us that the background brightness is equivalent to the one that we will get if there was one  $m = 20$  star per each square arc second (Sobrinho, 2014).

In order to convert values in msas to photons per second per pixel we can proceed as follows:

$$S_{sky}(s) = S_{obj}(s) \frac{A_{as}}{A_{pix}} \quad (11)$$

where  $S_{obj}(s)$  represents the number of photons per second that we will get from a single star with  $m = s$  (see Section 3.1),  $A_{as}$  is the area of the CCD in square arc seconds, and  $A_{pix}$  the area of the CCD in square pixels.

In order to convert this value into electrons we may use the expression:

$$N_{sky} = S_{sky} \times t \times QE \times n_{pix} \quad (12)$$

where  $t$  is the exposure time and  $n_{pix}$  represents the size of the object in pixels. If  $n_{pix} < 9$  then it is recommended to consider  $n_{pix} = 9$  (ETC , 2023).

- **Example (cont.):** At Pico do Juncal, quite near the SST observatories, we have, according to the measurements conducted in the year 2009,  $s \approx 20$  msas (Andrade, 2009). Evaluating  $S_{obj}$  for a  $m = 20$  star we get a flux of  $\approx 74.65$ phs<sup>-1</sup> (cf. Table 13). The areas associated with the CCD attached to the surveillance telescope are  $A_{as} = 9612 \times 9612 \approx 9.24 \times 10^7$  sas and  $A_{pix} = 4096 \times 4096 = 16777216$  square pixels. Inserting this values into equation (11) we get  $S_{sky} \approx 411.08$  phs<sup>-1</sup>pix<sup>-1</sup>.

For an exposure time of 10 s, a quantum efficiency of 73% and  $n_{pix} = 9$  we get  $N_{sky} = 411.08 \times 10 \times 0.73 \times 9 \approx 27008$  electrons.

We have proceeded this same way for different values of  $s$  ranging from 16 msas (full moon and/or lots of light pollution) to 23 msas (very dark sky). The results are compiled on Table 14.

### 3.3 Dark Current

The dark current for a CCD ( $S_{dark}$ ) is usually specified as the number of thermal electrons generated per second per pixel by the CCD itself. At room temperature the dark current of a typical CCD could be as high as  $\sim 10^4$  electrons per second per pixel. Typical values for properly cooled devices could be as low as 0.01 electrons per second per pixel (Howell, 2000).

In order to convert the value of  $S_{dark}$  from  $e^{-}s^{-1}pix^{-1}$  into electrons we may use the expression:

$$N_{dark} = S_{dark} \times t \times n_{pix} \quad (13)$$

where, as always,  $t$  is the exposure time and  $n_{pix}$  ( $\geq 9$ ) represents the size of the object in pixels.

- **Example (cont.):** The dark current associated with the CCD attached to the surveillance telescope is  $S_{dark} = 12.2e^{-}s^{-1}pix^{-1}$ . For an exposure time of 10 s and considering  $n_{pix} = 9$  we get  $N_{dark} = 12.2 \times 10 \times 9 = 1098$  electrons.

### 3.4 Read noise

The read noise values are normally expressed in units of electrons per pixel. For example a CCD with  $R_{pix} = 10e^{-}pix^{-1}$  means that in each read the CCD generates 10 electrons per pixel. Notice that the read noise does not depend on the exposure time (Howell, 2000).

In order to convert  $R_{pix}^2$  into electrons we just need to multiply it by the number of effective pixels:

$$R^2 = R_{pix}^2 n_{pix} \quad (14)$$

- **Example (cont.):** The read noise of the CCD attached to the surveillance telescope is, according to the manufacturer, 3.7 electrons per pixel. Thus, the contribution from the read noise to the total noise is  $R^2 = 3.7^2 \times 9 \approx 123$  electrons.

### 3.5 The CCD equation

Inserting equations (10), (12), (13) and (14) into equation (3) we get the so-called CCD equation:

$$SNR = \frac{S_{obj} \times t \times QE}{\sqrt{S_{obj} \times t \times QE + S_{sky} \times t \times QE \times n_{pix} + S_{dark} \times t \times n_{pix} + R^2 \times n_{pix}}} \quad (15)$$

- **Example (cont.):** Inserting all the obtained values into equation (15) we get:

$$SNR = \frac{3438}{\sqrt{3438 + 27008 + 1098 + 123}} \approx 19 \quad (16)$$

which means that we have a reasonable SNR value to start doing observations of the object with the surveillance telescope and taking 10 s of exposure time.

These calculations were performed for some observable SSSBs during the summer of 2023 resulting in the values seen in Table 15 and Table 16 for the surveillance and tracking telescopes, respectively.

Table 15: Calculations of the SNR values and respective exposure times, for the surveillance telescope, of some observable SSSBs during the summer of 2023 with their respective coordinates and apparent magnitudes.

Name	RA	Dec	m	t(s)	SNR
3753 Cruithne	03 15 42.7	+00 13 45	16.4	1.2	25
2212 Hephaistos	03 10 04.8	+17 16 26	17.6	1.2	10.90
5143 Heracles	01 22 57.9	+17 25 20	14.8	1.2	65.73
4197 Morpheus	22 20 02.3	-23 17 38	16.1	1.2	33.57
7092 Cadmus	01 41 45.8	-06 23 21	17.1	1.2	15.5
433 Eros	21 58 05.5	-09 31 55	10.3	1.2	812
887 Alinda	19 53 00.3	-22 14 29	10.0	1.2	812
10 Hygiea	21 30 43.1	-11 46 21	9.9	1.2	812

continues next page

**Table 15 – continuation**

<b>Name</b>	<b>RA</b>	<b>Dec</b>	<b>m</b>	<b>t(s)</b>	<b>SNR</b>
87 Sylvia	20 05 13.7	-31 37 09	11.7	1.2	318.8
52 Europa	17 36 41.7	-17 28 50	10.6	1.2	510.3
15 Eunomia	18 54 04.7	-24 34 48	8.3	1.2	2042.1
511 Davida	21 30 27.7	-24 18 21	10.5	1.2	510.3
50000 Quaoar	18 28 33.8	-15 05 47	18.7	15.0	9.82
174567 Varda	17 42 36.6	-01 39 01	20.1	120	11.15
38628 Huya	17 14 14.8	-07 03 44	19.5	120	11.15
469372	01 05 10.5	-04 49 15	21.9	120	1.8
47171	03 29 50.0	+12 51 15	19.9	120	11.15
617 Patroclus	22 17 37.4	-40 17 18	14.6	1.2	65.73
1867 Deiphobus	22 27 16.9	+17 55 44	15.5	1.2	33.57
1172 Aneas	23 20 15.8	+16 05 00	15.1	1.2	65.73
3317 Paris	23 52 41.2	-16 54 50	15.2	1.2	65.73
3451 Mentor	00 33 27.3	+04 27 21	15.0	1.2	65.73
4709 Ennomos	22 52 05.5	+24 06 30	15.7	1.2	33.57
136199 Eris	01 48 28.5	-00 38 38	18.6	15.0	9.82
225088 Gonggong	22 29 49.7	-10 47 13	21.4	120	0.04
303775	01 47 43.9	-01 16 38	21.3	120	0.04
589683	23 55 36.6	-21 50 26	21.3	120	0.04
523794	00 41 51.2	+07 21 39	21.8	120	1.8
42301	02 37 14.4	+16 08 07	21.6	120	1.8
523639	00 42 50.4	-08 33 34	21.2	120	0.04
55636	01 55 22.7	+38 32 40	20.0	120	11.15
307261	19 01 44.2	-05 30 25	20.3	120	11.15
Pluto	20 06 17.4	-23 00 44	15.0	1.2	65.73
16960	21 36 55.7	+06 34 59	15.1	1.2	65.73
4953	19 57 37.0	-52 39 09	15.2	1.2	65.73

Table 16: Calculations of the SNR values and respective exposure times, for the tracking telescope, of some observable SSSBs during the summer of 2023 with their respective coordinates and apparent magnitudes.

<b>Name</b>	<b>RA</b>	<b>Dec</b>	<b>m</b>	<b>t(s)</b>	<b>SNR</b>
3753 Cruithne	03 15 42.7	+00 13 45	16.4	1.2	47.63
2212 Hephaistos	03 10 04.8	+17 16 26	17.6	1.2	9.54
5143 Heracles	01 22 57.9	+17 25 20	14.8	1.2	92.49
4197 Morpheus	22 20 02.3	-23 17 38	16.1	1.2	47.63
7092 Cadmus	01 41 45.8	-06 23 21	17.1	1.2	22.15
433 Eros	21 58 05.5	-09 31 55	10.3	1.2	1127.7
887 Alinda	19 53 00.3	-22 14 29	10.0	1.2	1127.7
10 Hygiea	21 30 43.1	-11 46 21	9.9	1.2	1127.7
87 Sylvia	20 05 13.7	-31 37 09	11.7	1.2	443.52
52 Europa	17 36 41.7	-17 28 50	10.6	1.2	709.38
15 Eunomia	18 54 04.7	-24 34 48	8.3	1.2	2837.52
511 Davida	21 30 27.7	-24 18 21	10.5	1.2	709.38
50000 Quaoar	18 28 33.8	-15 05 47	18.7	15.0	40.64
174567 Varda	17 42 36.6	-01 39 01	20.1	120	15.88
38628 Huya	17 14 14.8	-07 03 44	19.5	120	15.88

continues next page

Table 16 – continuation

Name	RA	Dec	m	t(s)	SNR
469372	01 05 10.5	-04 49 15	21.9	120	2.54
47171	03 29 50.0	+12 51 15	19.9	120	15.88
617 Patroclus	22 17 37.4	-40 17 18	14.6	1.2	92.49
1867 Deiphobus	22 27 16.9	+17 55 44	15.5	1.2	47.63
1172 Aneas	23 20 15.8	+16 05 00	15.1	1.2	92.49
3317 Paris	23 52 41.2	-16 54 50	15.2	1.2	92.49
3451 Mentor	00 33 27.3	+04 27 21	15.0	1.2	92.49
4709 Ennomos	22 52 05.5	+24 06 30	15.7	1.2	47.63
136199 Eris	01 48 28.5	-00 38 38	18.6	15.0	40.64
225088 Gonggong	22 29 49.7	-10 47 13	21.4	120	6.36
303775	01 47 43.9	-01 16 38	21.3	120	6.36
589683	23 55 36.6	-21 50 26	21.3	120	6.36
523794	00 41 51.2	+07 21 39	21.8	120	2.54
42301	02 37 14.4	+16 08 07	21.6	120	2.54
523639	00 42 50.4	-08 33 34	21.2	120	6.36
55636	01 55 22.7	+38 32 40	20.0	120	15.88
307261	19 01 44.2	-05 30 25	20.3	120	15.88
Pluto	20 06 17.4	-23 00 44	15.0	1.2	92.49
16960	21 36 55.7	+06 34 59	15.1	1.2	92.49
4953	19 57 37.0	-52 39 09	15.2	1.2	92.49

## 4 A first observing program of SSSBs

With the objective of testing the observation and tracking of SSSBs using the SST telescopes, we created a list with nine of the objects presented in Tables 15 and 16 (See Table 17).

Among these nine SSSBs we have three Inner Solar System Asteroids (4197 Morpheus, 433 Eros, 887 Alinda), three Main Belt asteroids (10 Hygiea, 87 Sylvia, 52 Europa), the TNO Quaoar and the dwarf planets Eris and Pluto.

The objective was to use the surveillance telescope in order to obtain images of these objects during a few days or weeks and analyze the respective trail against the background stars.

## 5 Discussion and conclusions

Although the two SST telescopes installed at Pico do Areeiro are configured to detect and track space debris in Earth’s orbit they can be used also in terms of Observational Astronomy. In this work we explored the possibility of using these equipments in order to observe and track SSSBs. In particular we have considered the observation of asteroids (Atiras, Amors, Atens, Apollos, Main Belt, Trojans), Centaurs and TNOs. We also considered dwarf planets and PHAs.

We started by listing the brightest objects belonging to each group (Tables 2 - 11) and then we consider a selection of the objects observable during the Summer of 2023 (Tables 15 and 16). For each one of these we determined the exposure time and the associated SNR value. We did this for both telescopes. As a result we find out that the brightest SSSBs ( $m < 18$ ) can be observed with both telescopes with exposure times of  $\sim 1$  s at very reasonable SNR values ( $\text{SNR} > 10$ ). SSSBs with  $m > 20$  demand exposures times of  $\sim 100$  or higher. In order to illustrate this we present the following examples:

- **15 Eunomia** (Main Belt asteroid) – for an exposure time of 1.2 s we get a SNR of  $\sim 10^3$  for both telescopes meaning that the observation can be performed in excellent conditions.

Table 17: Proposed list of observable SSSBs along with the coordinates during July 2023, their apparent magnitudes and proposed exposure times.

Name	Dec	RA	m	t(s)
4197 Morpheus	22 20 02.3	-23 17 38	16.1	1.2
433 Eros	21 58 05.5	-09 31 55	10.3	1.2
887 Alinda	19 53 00.3	-22 14 29	10.0	1.2
10 Hygiea	21 30 43.1	-11 46 21	9.9	1.2
87 Sylvia	20 05 13.7	-31 37 09	11.7	1.2
52 Europa	17 36 41.7	-17 28 50	10.6	1.2
50000 Quaoar	18 28 33.8	-15 05 47	18.7	15
136199 Eris	01 48 28.5	-00 38 38	18.6	15
Pluto	20 06 17.4	-23 00 44	15.0	1.2

- **2212 Hephaistos** (second largest Apollo asteroid) – for an exposure time of 1.2 s we get  $\text{SNR} \approx 10$  meaning that the conditions are sufficient to do the observation.
- **50000 Quaoar** (the 7th TNO in size) – in order to get  $\text{SNR} \approx 10$  the exposure time should be  $\approx 15$  s.
- **174567 Varda** (the 9th TNO in size) – with an exposure time of 120 s we get  $\text{SNR} \approx 11.15$  (surveillance telescope) and  $\text{SNR} \approx 15.88$  (tracking telescope) which means that in these conditions the observation is possible with both telescopes.
- **225088 Gonggong** (the 5th TNO in size) - even with an exposure time of 120 s we get  $\text{SNR} \approx 0.04$  (surveillance telescope) and  $\text{SNR} \approx 6.36$  (tracking telescope) which means that it will be not possible to observe this object without extending significantly the exposure time (specially in the case of the surveillance telescope).

We presented an observation proposal for nine of the considered objects (Table 17). Unfortunately it was not possible to accomplish the proposed observations before the end of this internship (Estágios de Verão 2023).

Nevertheless it is our conclusion that the capabilities of the SST equipments are well enough to observe and track asteroids, TNOs and dwarf planets as well. In terms of future work we intend to:

- Perform the observations listed in Table 17 (or equivalent) and analyze the obtained results;
- Consider the use of SST telescopes to track Near Earth Objects;
- Consider the use of SST telescopes to observe fainter SSSBs;
- Consider the use of SST telescopes to observe and track comets.

We should consider the values of exposure time proposed in Table 17 as guidelines, and if any observations were to be carried out, these values should be compared to those of Tables 15 and 16 and should be adjusted as needed.

## A Magnitude

The absolute magnitude  $M$  is a measure of the luminosity of a celestial body. It is commonly defined as the apparent magnitude  $m$  that the object would have if it were viewed from a distance of 10 pc (without interstellar extinction of its light). The relation between the two magnitudes  $M$  and  $m$  is given by equation (4). For Solar System bodies such as planets and asteroids a more suitable definition for absolute magnitude is used. In this case the absolute magnitude, represented by  $H$ , is defined as the apparent magnitude that the solar system object would have if it is located at a distance of 1 AU away from both the observer and the Sun, and in conditions of solar opposition. Because solar system bodies shine as they are illuminated by the Sun their brightness  $m$  varies with time, more precisely as a function of the phase angle  $\alpha$ , the angle between observer, sun and the solar system body. The relation between  $H$  and  $m$  is now given by (Maeda et al., 2021):

$$m = H + 5 \log \left( \frac{R\Delta}{D^2} \right) - q(\alpha) \quad (17)$$

where  $R$  is the heliocentric distance to the solar system body,  $D$  is the heliocentric distance to the observer (1 AU for an observer located on the surface of the Earth),  $\Delta$  is the distance between the observer and the solar system body and  $q(\alpha)$ , termed the *phase function*, is given by (Maeda et al., 2021):

$$q(\alpha) = -2.5 \log [(1 - G)\Phi_1(\alpha) + G\Phi_2(\alpha)] \quad (18)$$

where  $G$  is called the *slope parameter*. The value of  $G$  is not known for most asteroids. A value of  $G \approx 0.15$  is assumed in general, although  $G$  could assume very different values (in rare cases we could even have  $G < 0$ ).  $\Phi_1$  and  $\Phi_2$  are functions of the phase angle  $\alpha$  such that (Maeda et al., 2021):

$$\Phi_1(\alpha) = \exp \left( -A_1 \left( \tan \frac{\alpha}{2} \right)^{B_1} \right) \quad (19)$$

and

$$\Phi_2(\alpha) = \exp \left( -A_2 \left( \tan \frac{\alpha}{2} \right)^{B_2} \right) \quad (20)$$

with  $A_1 = 3.33$ ,  $A_2 = 1.87$ ,  $B_1 = 0.63$  and  $B_2 = 1.22$ .

The relation between the distances  $R$ ,  $D$ ,  $\Delta$  and the phase angle  $\alpha$  is given by (see Figure 1):

$$\cos(\alpha) = \frac{\Delta^2 + R^2 - D^2}{2R\Delta} \quad (21)$$

## References

Andrade I., 2009, *Medições do Seeing em oito locais da ilha da Madeira e seu estudo comparativo*, Relatório do projecto de fim de curso da licenciatura em Engenharia de Instrumentação e Electrónica (Ramo de Astronomia), Universidade da Madeira, pp.209.

Dhillon V., 2010, *Astronomical Techniques*, University of Sheffield, [http://www.vikdhillon.staff.shef.ac.uk/teaching/phy217/detectors/phy217\\_det\\_noise.html](http://www.vikdhillon.staff.shef.ac.uk/teaching/phy217/detectors/phy217_det_noise.html)

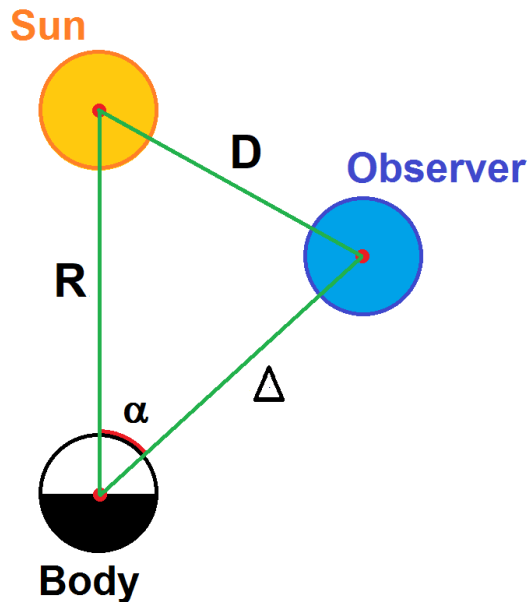


Figure 1: The phase angle diagram (adapted from Renerpho 2019, [https://en.wikipedia.org/wiki/Absolute\\_magnitude/media/File:Phase\\_angle\\_explanation.png](https://en.wikipedia.org/wiki/Absolute_magnitude/media/File:Phase_angle_explanation.png))

EMCCD 201, EMCCD Microscope Cameras and Detectors, Oxford Instruments 2023, [https://andor.oxinst.com/products/emccd-cameras?gclid=CjwKCAjw5M01BhBTEiwAAJ8e1qJsCVeVJ5bueaf86c52aSTs-A\\_y5rss1yk3elt0bqon4hfhzIXQvhoCcpEQAvD\\_BwE](https://andor.oxinst.com/products/emccd-cameras?gclid=CjwKCAjw5M01BhBTEiwAAJ8e1qJsCVeVJ5bueaf86c52aSTs-A_y5rss1yk3elt0bqon4hfhzIXQvhoCcpEQAvD_BwE)

The Basics of the Exposure Time Calculator, Lowell Observatory, <http://www2.lowell.edu/rsch/LMI/ETCMethod.pdf>

Freitas J. et al., 2021, *Portuguese SST capability - The Portuguese Space Surveillance network system*, Proc. 8th European Conference on Space Debris (virtual), Darmstadt, Germany, 20-23 April 2021, published by the ESA Space Debris Office Ed. T. Flohrer, S. Lemmens & F. Schmitz, <http://conference.sdo.esoc.esa.int,May2021>.

GSENSE4040, 2023, Gpixel Inc. <https://www.gpixel.com/products/area-scan-en/gsense/gsense4040/>

Hainaut O., 2005, *Signal, Noise and Detection*, ESO, <http://www.sc.eso.org/~ohainaut/ccd/sn.html>.

Howell S. B., 2000, *Handbook of CCD Astronomy*, Cambridge University Press, London, ISBN 0 521 64834 3.

Resolution B5 - *Definition of a Planet in the Solar System*, 2006, International Astronomic Union.

Maeda N. et al., 2021 *Size distributions of bluish and reddish small main-belt asteroids obtained by Subaru/Hyper Suprime-Cam*, AJ, 162, 280.

Minor Planet Center, International Astronomic Union, 2023, <https://www.minorplanetcenter.net/>

Sobrinho J. L. G., 2014, *Poluição Luminosa*, Astronomia no Verão 2014, Universidade da Madeira.

Sobrinho J. L. G., 2022, *Potencial astronómico das imagens SST*, Relatório sobre a eventual exploração astronómica das imagens obtidas no âmbito do projecto Space Surveillance and Tracking (SST), 14pp; Universidade da Madeira.